ADVANCES IN ATMOSPHERIC SCIENCES, VOL. 24, NO. 5, 2007, 927–938

Development of a Model for Water and Heat Exchange Between the Atmosphere and a Water Body

SUN Shufen*[1] (孙菽芬), YAN Jinfeng[2] (颜金凤), XIA Nan[2] (夏 南), and SUN Changhai[2] (孙长海)

[1] *State Key Laboratory of Numerical Modeling for Atmospheric Sciences and Geophysical Fluid Dynamics* (*LASG*), *Institute of Atmospheric Physics, Chinese Academy of Sciences, Beijing* 100029

[2] *Shanghai Institute of Applied Mathematics and Mechanics, Shanghai University, Shanghai* 200072

(Received 10 September 2006; revised 12 February 2007)

ABSTRACT

A model for studying the heat and mass exchange between the atmosphere and a water body is developed, in which the phase change process of water freezing in winter and melting in summer and the function of the convective mixing process are taken into consideration. The model uses enthalpy rather than temperature as the predictive variable. It helps to set up governing equations more concisely, to deal with the phase change process more easily, and make the numerical scheme simpler. The model is verified by observed data from Lake Kinneret for a non-frozen lake in summer time, and Lake Lower Two Medicine for a frozen lake in winter time. Reasonably good agreements between the model simulations and observed data indicate that the model can serve as a component for a water body in a land surface model. In order to more efficiently apply the scheme in a climate system model, a sensitivity study of various division schemes with less layers in the vertical direction in the water body is conducted. The results of the study show that the division with around 10 vertical layers could produce a prediction accuracy that is comparable to the fine division with around 40 layers.

Key words: water body model, enthalpy, convective mixing, model validation

DOI: 10.1007/s00376-007-0927-7

1. Introduction

Inland water bodies such as lakes and reservoirs occupy small percentage of the world continent but are important part of the continental land surface. Evaporation is a primary path for water loss from these bodies and can modify the properties of air masses passing over them. Compared with land surfaces covered by vegetation, bare soil etc., water bodies have quite different properties of albedo, heat capacity, transport of turbulent fluxes to the atmosphere, and so on, and they play an important role in the climate system, particularly at local and regional scales. However, considering the very coarse grid sizes used in previous global general circulation models (GCMs), the sizes of many inland water bodies are too small to have been identified at such coarse resolutions. Therefore, most second generation land surface models (LSMs), such as BATS (Dickinson et al., 1993), SiB (Sellers et al., 1986) and others did not take inland water bodies into consideration. Recently, however, due to fast progress in computer capabilities, which has promoted the development of mosaic LSMs to deal with sub-grid heterogeneity in global LSMs, reducing the grid size in current regional climate models to around 10^3 km^2, inclusion of inland water bodies in LSM model has become more and more important. Indeed, some recently developed land surface models (Bonan, 1996; Oleson et al., 2004) have acknowledged this by taking water bodies into consideration as an important underlying land surface.

Since the scale of water bodies concerned in current LSMs is still more than 100 km^2, sub-models for water bodies are one dimensional, using the turbulent eddy diffusion mechanism and Fourier's Law to treat heat transfer inside the water body. Since the 1980s and earlier, many models for inland water bodies have been developed, and these provide instructive

*Corresponding author: SUN Shufen, ssf@lasg.iap.ac.cn

knowledge and useful reference for the model developed here. However, there is still room for improvement. First, there are only a few models that consider the coexistence of two phases of water and deal with the phase change between liquid and ice (Hostetler and Bartlein, 1990; Liston and Hall, 1995a; Fang and Stefan, 1996; Stefen and Fang, 1997); most mainly describe the heat balance processes for either a liquid water body (Henderson-Sellers, 1985; Henderson-Sellers, 1986; Zhou and Chapra, 1997; Bonan, 1996; Oleson et al., 2004; Bell et al., 2006) or a frozen (ice/snow) water body (Hostetler, 1991; Vavrus et al., 1996; Patrick et al., 2002). Furthermore, they do not deal with freezing and melting processes which occur very often in high latitude or in mountainous areas, such as the Tibetan Plateau. Second, most of the models do not include thermal convective mixing mechanisms, except for a few proposed by Hostetler and Bartlein (1990) in which liquid water density in the surface layer is heavier than that in the adjacent layer below. Mixing plays an important role in regulating the surface temperature and, in turn, turbulent fluxes to the atmosphere. Finally, almost all the models use temperature as the predictive variable, which is not convenient for describing the system of liquid and ice coexistence with phase change processes.

In this paper, an improved model for the water body system is developed, which describes phase change processes of the water body through the formulation of physical-based models, accounting for the various relevant processes occurring within, and at the boundaries of, the liquid water, ice, snow and atmospheric components of the natural system. It can, in principle, be applied to both deep (around 50 m) and shallow (around 10 m) water bodies. The models of liquid water, ice and snow (1) consider the phase change processes between ice and liquid water, (2) take the convective mixing process at the interface between two adjacent layers of liquid water into consideration, (3) use enthalpy rather than temperature as the predictive variable in their energy balance equations, and (4) develop an efficient numerical scheme for the enthalpy equations, which can easily handle icing and melting processes in the water body.

In section 2, basic equations governing the energy balance of the entire water body system are presented. In section 3, the efficient numerical scheme is described. The model is verified by using observation data from the deep lakes of Kinneret and Lower Two Medicine in section 4, and in section 5 simplification of the model by reducing the number of vertical layer divisions in the water is discussed. A summary and conclusions are presented in section 6.

2. Governing equations of energy balance

Water body energy balance is governed by solar radiation, longwave radiation down from the atmosphere and up from the water body surface, latent heat and sensible heat flux exchanges between the water body and atmosphere, heat conduction within the water body, and energy absorbed/released due to phase changes inside the water body. A water body system can consist of liquid water, ice, and possibly snow, if it has fallen on top of any ice cover. In order to better handle the complicated freezing/melting processes in the energy balance, enthalpy will be used as the predicted variable in the current model, which helps to establish a more functional numerical scheme. Since it is very possible for liquid water to form unstable temperature stratification profiles at night, in winter, and in spring, and that these unstable profiles cannot last for long periods of time, the convective mixing mechanisms between liquid layers is applied to smooth the temperature profile between the unstable stratification layers.

2.1 *Energy balance equations for liquid water, ice and snow*

In most currently used models for liquid water (Hostetler and Bartlein, 1990; Fang and Stefan, 1996; Stefen and Fang, 1997; Bonan, 1996; Oleson et al., 2004), the one-dimensional energy balance equation is often written as:

$$\frac{\partial T}{\partial t} = -\frac{1}{A(z)}\frac{\partial}{\partial z}\left\{A(z)[d_{\mathrm{m}} + D(z,t)]\frac{\partial T}{\partial z}\right\} + \frac{1}{A(z)}\frac{1}{C_{\mathrm{w}}}\frac{\partial[\phi A(z)]}{\partial z}, \tag{1a}$$

where T is water temperature (K), t is time (s), z is depth from the surface (m), $A(z)$ is the area of liquid water (m^2) at depth z, d_{m} is the molecular heat diffusivity coefficient of water ($\mathrm{m}^2\ \mathrm{s}^{-1}$), $D(z,t)$ is the heat diffusivity coefficient of water ($\mathrm{m}^2\ \mathrm{s}^{-1}$) due to turbulent eddy mixing, and ϕ is the heat source term ($\mathrm{W\ m}^{-2}$), such as that from solar radiation. C_{w} is heat capacity of water ($\mathrm{J\ m}^{-3}$). Equation (1) does not consider the phase change of liquid water as well as the convective mixing mechanism. In order to deal with the phase exchange influence and also to take the mixing effect into account, for a water body with constant $A(z)$, Eq. (1) should be modified into the two following equations:

$$\frac{\partial T}{\partial t} = \frac{\partial}{\partial z}\left\{[d_{\mathrm{m}} + D(z,t)]\frac{\partial T}{\partial z}\right\} +$$

$$\frac{1}{C_{\rm w}}\frac{\partial\phi}{\partial z}+L_{\rm il}\rho_{\rm l}\frac{\partial f_{\rm ice}}{\partial t}+M_{\rm conv}\ , \tag{1b}$$

where $L_{\rm il}\rho_{\rm l}\partial f_{\rm ice}/\partial t$ is the phase change energy released/absorbed when liquid water/ice becomes ice/liquid and temperature is equal to freezing point ($T_{\rm f}=273.15$ K); $L_{\rm il}$ is the specific fusion heat of water (3.336×10^5 J kg^{-1}) and $f_{\rm ice}$ is the mass fraction of ice in the total water equivalent; $\rho_{\rm l}$ is the density of liquid water (1000 kg m^{-3}); and the term of $M_{\rm conv}$ represents convective mixing, one which only functions when heavier liquid lays over lighter liquid, and the reason for including this term will be explained later. In real situations, during the freezing/melting processes, T remains equal to $T_{\rm f}$, and the numerical scheme must shift to another equation to solve $f_{\rm ice}$. However, Eq. (1b) is not suitable, because, in using this equation to numerically calculate T, T will oscillate around 0°C, and it is hard to keep 0°C stable during the freezing/melting period. In order to avoid this, however, enthalpy can be used. Enthalpy varies monotonically during the phase-change process. Therefore, the numerical scheme can solve the continuous phase-change process from water/ice to ice/water smoothly, and then use the calculated enthalpy value to determine the various values of $f_{\rm ice}$. In the model developed here, the energy balance equation for the enthalpy is given by:

$$\frac{\partial h}{\partial t}=\frac{\partial}{\partial z}\left\{[k+K(z,t)]\frac{\partial T}{\partial z}\right\}-\frac{\partial\phi}{\partial z}+M_{\rm conv}\ , \tag{2}$$

where h (J m^{-3}) of the water body is the volumetric enthalpy, defined as:

$$\begin{aligned}h=&[(1-f_{\rm ice})\times c_{\rm l}\times(T-T_{\rm f})+\\&f_{\rm ice}\times(T-T_{\rm f})-f_{\rm ice}\times L_{\rm il}]\times\rho_{\rm l}\ .\end{aligned} \tag{3a}$$

The nonlinear equation (Eq. (2)) associated with Eq. (3a) can be solved more easily. In these equations, the enthalpy of liquid water at the freezing temperature $T_{\rm f}=273.15$ K is defined as zero, $c_{\rm l}$ is the specific heat of water (4188 J kg^{-1} K^{-1}), $c_{\rm ice}$ is the specific heat of ice (2052 J kg^{-1} K^{-1}), k is molecular thermal conductivity (W m^{-1} K^{-1}), and $K(z,t)$ is thermal conductivity due to turbulent eddies (W m^{-1} K^{-1}). For liquid water, $k=k_{\rm l}=d_{\rm m}\times C_{\rm w}=0.6$ W m^{-1} K^{-1}, $K(z,t)=K_{\rm l}=D(z,t)\times C_{\rm w}$ [$K(z,t)$ will be estimated in section 2.3]. Equation (2) can also apply to possible ice or snow case except that $k=k_{\rm ice}=2.034$ W m^{-1} K^{-1} for ice and $k=k_{\rm snow}=f(\rho_{\rm snow})$ for snow ($\rho_{\rm snow}$ is the snow density and assumed to be constant (2000 kg m^{-3}) in this model. For both ice and snow, the terms $M_{\rm conv}$ and $K(z,t)=0$. ϕ (later uses the symbol $s_{\rm n}$) (J m^{-2} s^{-1}) is estimated by Eq. (12) based on Bear's Law. A water body consisting of liquid water, ice and snow will be divided into layers for difference scheme of Eq. (2) later, and the enthalpy for each layer with thickness $\Delta z, h_{\rm L}$, is given by:

$$\begin{aligned}h_{\rm L}=&m_{\rm liq}\times c_{\rm l}\times(T_{\rm liq}-T_{\rm f})+m_{\rm ice}\times\\&c_{\rm ice}\times(T_{\rm ice}-T_{\rm f})-m_{\rm ice}\times L_{\rm il}\ ,\end{aligned} \tag{3b}$$

or

$$\begin{aligned}h_{\rm L}=&m_{\rm total}\times(1-f_{\rm ice})\times c_{\rm l}\times(T_{\rm liq}-T_{\rm f})+\\&m_{\rm total}\times f_{\rm ice}\times c_{\rm ice}\times(T_{\rm ice}-T_{\rm f})-\\&m_{\rm total}\times f_{\rm ice}\times L_{\rm il}\ ,\end{aligned} \tag{3c}$$

$$h_{\rm L}=h\cdot\Delta z\ , \tag{3d}$$

where $m_{\rm liq}, m_{\rm ice}$ and $m_{\rm total}=m_{\rm ice}+m_{\rm liq}$ (kg) are liquid water mass, ice mass, and total mass in the layer, respectively; and $f_{\rm ice}$ is the mass fraction of ice $m_{\rm ice}$ to total mass $m_{\rm total}$ in the layer. For a layer with a mixture of liquid water and ice, k and $K(z,t)$ are estimated by $k=(1-f_{\rm ice})\times k_{\rm l}+f_{\rm ice}\times k_{\rm ice}$ and $K=(1-f_{\rm ice})\times K_{\rm l}+f_{\rm ice}\times K_{\rm ice}$ in this model.

Two equations [Eq. (2) and Eqs. (3b) or (3c)] for $h_{\rm L}$ contain three unknown variables ($h_{\rm L}, T, f_{\rm ice}$). One more condition is needed to make the system close more robust, and the condition comes from the following constraint:

$$\text{If}\begin{cases}h_{\rm L}>0 & \Rightarrow T>0 \text{ and } f_{\rm ice}=0.0\\ -m_{\rm total}L_{\rm il}<h_{\rm L}<0 & \Rightarrow T=T_{\rm f} \text{ and } 0.0<f_{\rm ice}<1.0\\ h_{\rm L}<-m_{\rm total}L_{\rm il} & \Rightarrow T<T_{\rm f} \text{ and } f_{\rm ice}=1.0\end{cases} \tag{4}$$

2.2 *Boundary conditions*

Equations (2)–(4) are hyperbolic equations and therefore need boundary conditions to obtain a real solution. There are two boundary conditions: upper surface boundary and lower boundary conditions.

The surface boundary conditions require thermal heat flux Q at the surface:

$$Q=-[k+K]\partial T/\partial z \quad \text{at} \quad z=0.0 \tag{5}$$

is equal to the net incoming heat flux at the lake surface (W m^{-2}):

$$Q=S_{\rm n}+L_{\rm n}-H_{\rm s}-LE+R_{\rm p} \tag{6a}$$

or

$$-[k+K]\partial T/\partial z=S_{\rm n}+L_{\rm n}-H_{\rm s}-LE+R_{\rm p} \tag{6b}$$

where $S_{\rm n}$ is net absorbed shortwave radiation (W m^{-2}), $L_{\rm n}$ is net absorbed longwave radiation (W m^{-2}), $H_{\rm s}$ is the positive upward flux of sensible

heat (W m^{-2}), LE is the positive upward flux of latent heat (W m^{-2}) ($L = L_{\rm lv}$ when the water body surface is liquid or $L = L_{\rm iv}$ when the lake surface is frozen), E is the flux of evaporation (kg m^{-2} s^{-1}), and $R_{\rm p}$ is the heat flux brought by precipitation (W m^{-2}).

Since the water body depth is more than 10 m (depth of a deep water body is defined as more than 50 m and the depth of a shallow water body more than 10 m and lower than 50 m), the lower boundary conditions often use zero heat flux conditions at the bottom of the water body and are given by:

$$\frac{\partial T}{\partial z} = 0 \,. \tag{7}$$

2.2.1 *Latent heat and sensible heat*

In Eq. (6), the latent heat and sensible heat flux between the lake surface and atmosphere is estimated by Monin-Obukhov theory (Businger et al., 1971; Dyer, 1974):

$$H = \rho_{\rm a} c_p (\overline{w'\theta'}) = -\rho_{\rm a} c_p u_* \theta_* \tag{8}$$

$$LE = L\rho_{\rm a}(\overline{w'q'}) = -\rho_{\rm a} u_* q_* L \,, \tag{9}$$

where $\rho_{\rm a}$ is the air density (kg m^{-3}), c_p is the specific heat of dry air (J kg^{-1} K^{-1}), q_* is the humidity scale, u_* is the surface friction velocity (m s^{-1}), and θ_* is the turbulent temperature scale (K). The magnitude of u_*, θ_* and q_* can be estimated by an iteration procedure based on Monin-Obukhov theory.

2.2.2 *Water surface energy brought by precipitation*

The heat energy flux rate, $R_{\rm p}$, brought by precipitation only exists in the surface layer:

$$R_{\rm p} = \frac{p_{\rm rain} C_{\rm l}(T_{\rm prec} - T_{\rm f}) + p_{\rm snow} C_{\rm ice}(T_{\rm prec} - T_{\rm f}) - p_{\rm snow} L_{\rm il}}{\Delta t} \,, \tag{10}$$

where $p_{\rm rain}$ and $p_{\rm snow}$ indicate the rain and snow amounts (kg) in the time interval Δt (s), respectively; and $T_{\rm prec}$ is the precipitation temperature (K). In this model, the mass and energy held by the precipitation is assumed to be completely mixed with that held by the liquid water (or ice, or snow) in the surface layer, and the mixture will finally have unified enthalpy and temperature. The runoff from the mixture in the surface layer is determined in this model depending on the final temperature calculated by applying the constraints expressed in Eq. (4). If the temperature is less than $T_{\rm f}$, all the mass from the precipitation in the current time step will become ice, adding to the surface layer and increasing its thickness, and there will be no runoff from the surface layer. If the temperature is higher than $T_{\rm f}$, all liquid mass produced from the cumulative precipitation will become runoff, flowing away form the surface layer, with the surface layer thickness returning to its original state. If the temperature is equal to $T_{\rm f}$, all liquid water from the accumulated precipitation will become runoff and all ice from the accumulated precipitation will still stay in the surface layer and increase its thickness. In this model, for the sake of simplicity, snowfall is viewed as having constant density and will pile on top of the ice cover. In the future, a snow model developed by the authors (Sun et al., 1999) will be implemented into this model to overcome this weakness.

2.2.3 *Net longwave radiation*

Longwave radiation from air is mostly absorbed by the water body surface. The absorbed net longwave radiation is given by:

$$L_{\rm n} = \varepsilon L_{\rm a}^{\downarrow} - \varepsilon \sigma T_{\rm s}^4 \tag{11}$$

where $L_{\rm a}^{\downarrow}$ is the downward flux of radiation from air (W m^{-2}), $T_{\rm s}$ is the temperature of the water body surface (K), σ is the Stefan-Boltzmann constant ($\sigma = 5.67 \times 10^{-8}$ W m^{-2} K^{-4}), ε is the emissivity of the water body surface (in this model, $\varepsilon = 0.96$ if there is liquid water at the surface, or 0.98 if there is ice or snow at the surface).

2.2.4 *Shortwave radiation*

Since there may be a turbid substance in a thin layer of a water body below a possible snow layer which can absorb solar radiation, it is assumed that the turbid substance in the thin layer will collect the portion, β, of total shortwave radiation $S_{\rm n}^*$ absorbed by the water body below the snow layer. The turbid layer concentrates the solar radiation $S_{\rm n} = S_{\rm n}^* \times \beta$. Solar radiation below the turbid layer abides by Beer's Law and is given by:

$$S_{\rm n}(z) = S_{\rm n}^* \times (1 - \beta) \times \exp(-\lambda z) \tag{12a}$$

with $S_{\rm n}^*$ calculated as follows:

$$S_{\rm n}^* = S_{\rm n}(0)(1 - \alpha)\exp(-\lambda_{\rm s} z_{\rm snow}) \,, \tag{12b}$$

where $S_{\rm n}(0)$ is the total solar radiation reaching the water surface; $z_{\rm snow}$ is the snow layer thickness; α is the abledo of the water body surface [$\alpha = 0.06$ if there is liquid water at the surface, or α ranges from 0.15 to 0.3 (Patterson and Hamblin, 1988) if there is ice at the surface, or α ranges from 0.3 to 0.78 if there is snow cover at the surface.] It is a critical parameter that greatly influences the energy balance of the water body and in turn affects its temperature distribution, its phase change process, and its turbulent flux at the lake surface. λ is the extinction coefficient of the water body to shortwave radiation. In this model, λ equates

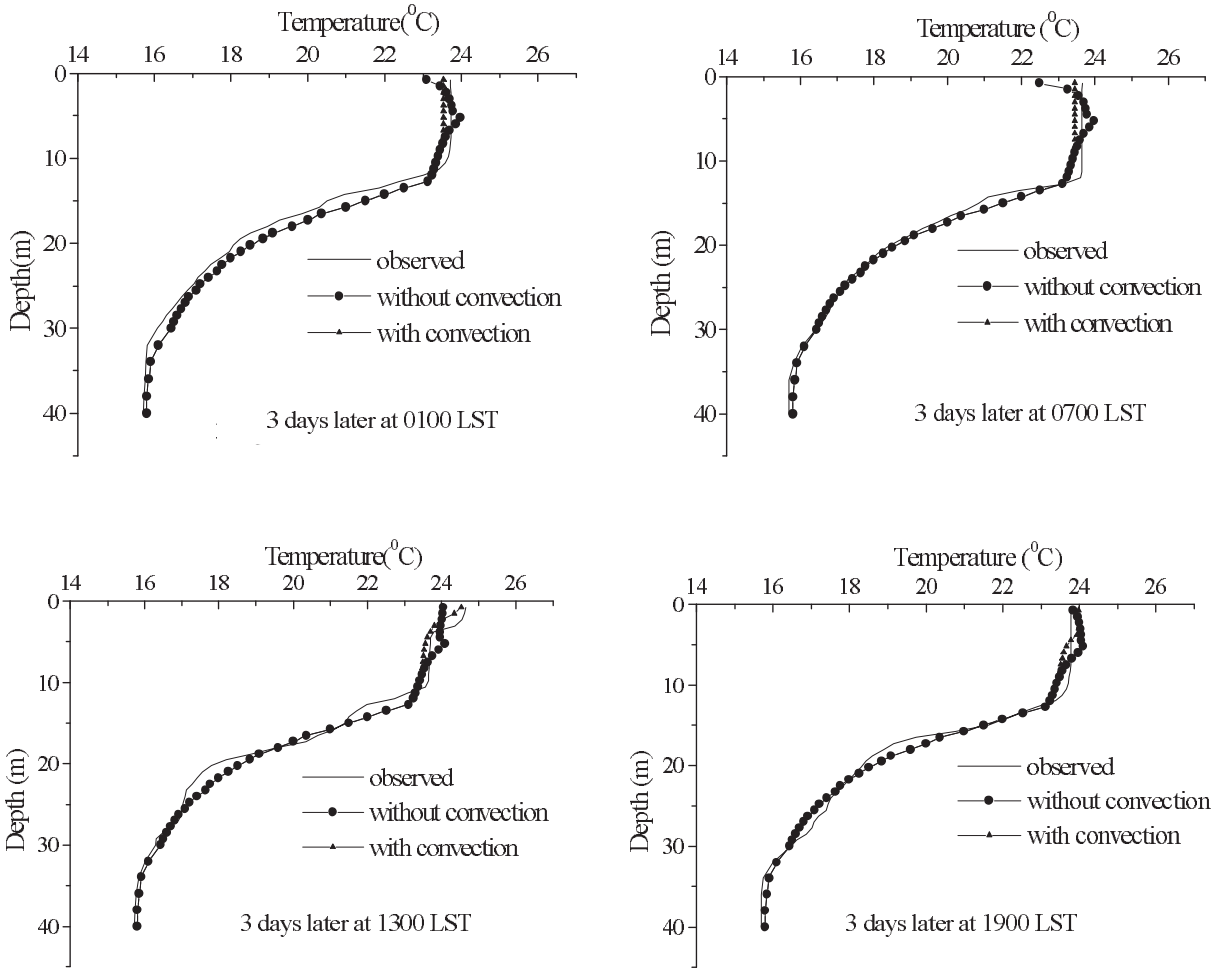

Fig. 1. Comparison of simulated and observed temperature profiles at different times on day three.

Table 1. Statistics of temperature differences between two schemes with and without the convective mixing process.

Depth (m)	0.75	1.5	2.25	3.0	3.75	4.5	5.25	6.0	6.75	7.5	8.25	9.0	9.75
Average (K)	0.32	0.15	0.20	0.30	0.42	0.48	0.57	0.59	0.41	0.21	0.07	0.02	0.0
Maximum (K)	1.19	0.82	0.68	0.68	0.78	0.89	1.07	1.11	0.94	0.53	0.17	0.04	0.01

to λ_l and they range from 0.5 to 1.0 m^{-1} for liquid water; $\lambda = \lambda_{ice} = 1.5$ m^{-1} for ice; and λ_s=6.0 m^{-1} for snow (Patterson and Hamblin, 1988).

2.3 *Parameter determination*

To simulate the turbulent thermal conductivity by eddies in liquid water, the method proposed by Henderson-Sellers (1985) is followed, which requires no lake-specific fitting of parameters. For shallow water bodies, liquid turbulent thermal conductivity is given by:

$$K(z) = 0 \tag{13a}$$

and for deep water bodies, it is given by:

$$K(z) = C_w \times (k_v w^* z / Pr_0) e^{(-k^* z)} (1 + 37 Ri^2)^{-1} \tag{13b}$$

where k_v is the von Karman constant (=0.4); Pr_0 is the neutral value of the turbulent Prandtl number (1.0); k^* is a latitude-dependent parameter of the Ekman profile; w^* (m s^{-1}) is the friction velocity at the surface, and is estimated by the wind speed at 2 m above the water's surface U_2 (m s^{-1}):

$$w^* = 1.2 \times 10^{-3} U_2 \ ,$$

k^* is determined from

$$k^* = 6.6 (\sin\theta)^{1/2} U_2^{-1.84} \ ,$$

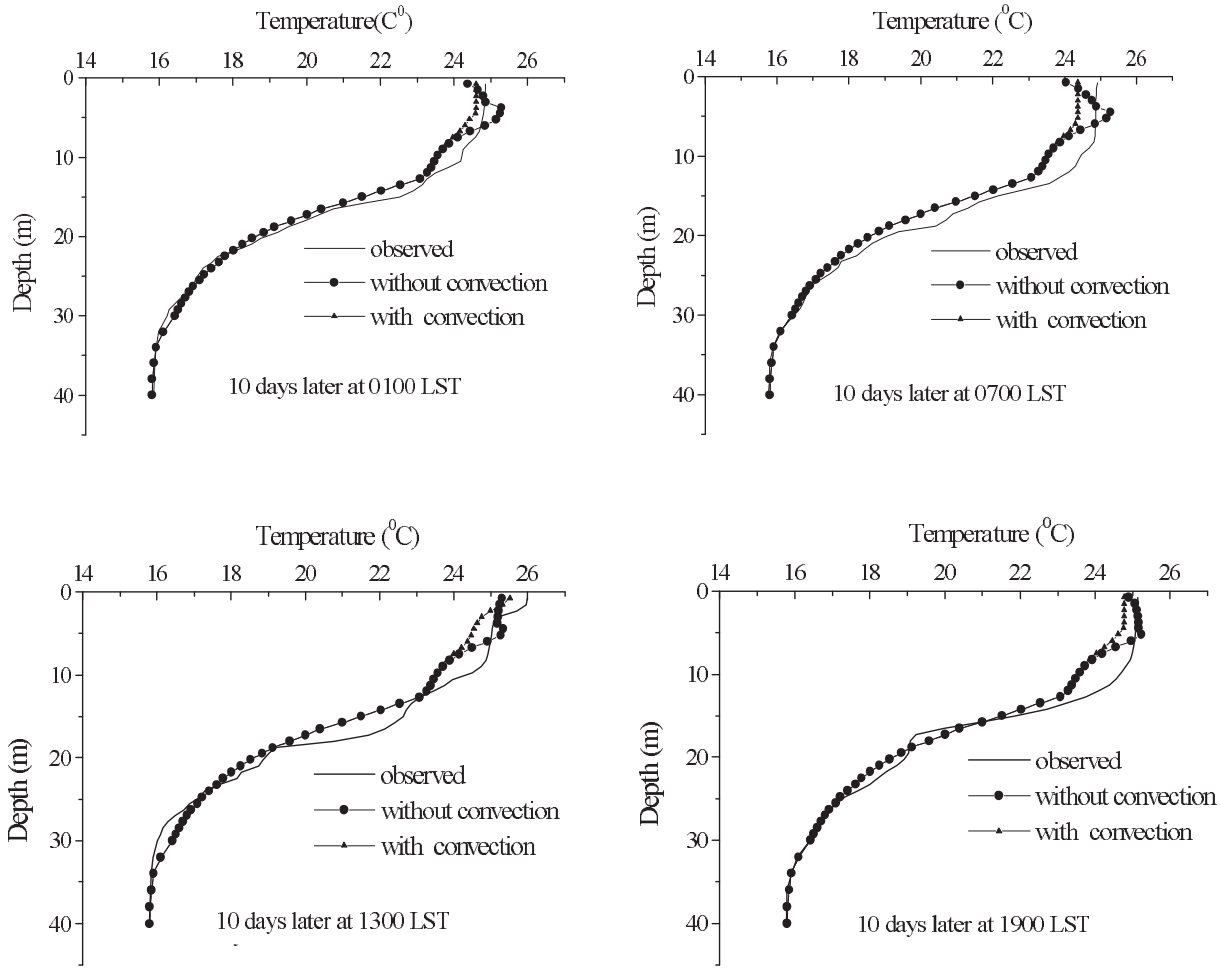

Fig. 2. Comparison of simulated and observed temperature profiles at different times on day 10.

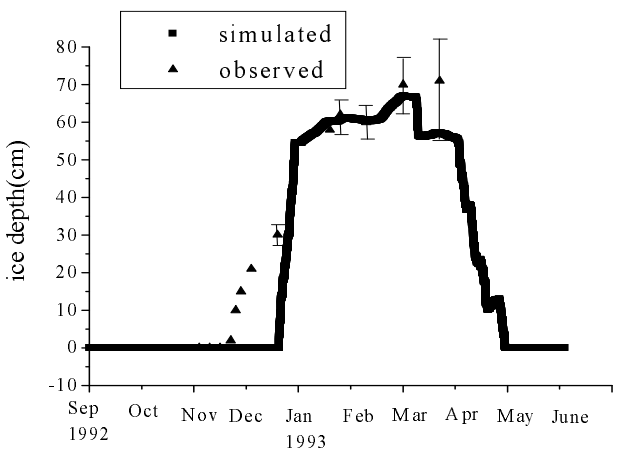

Fig. 3. Comparison of simulated and observed ice depths at different times.

where θ is the latitude of the water body being studied and Ri is the Richardson number, which is calculated by:

$$Ri = \frac{-1+\{1+40N^2k^2z^2/[w^{*2}\exp(-2k^*z)]\}^{1/2}}{20},$$

where N is the Brunt-Vaisala frequency, which is specified as:

$$N = [-g/\rho(\partial\rho/\partial z)]^{1/2}$$

and the density of fresh water ρ (kg m^{-3}) is given by the formula:

$$\rho = (1 - 1.9549 \times 10^{-5}|T - 277|^{1.68})10^3 . \qquad (14)$$

2.4 *Convective mixing scheme*

Although Hostetler and Bartlein (1990) and Liston and Hall (1995a) mentioned the convective mixing mechanism for unstable stratification of water density distribution, most currently used lake-type water body models do not take the mixing function into consideration. In reality, it is very unstable in a water body

when a water layer with a higher density is placed over one with a lower density. In the theory of absolute equilibrium, necessary and sufficient conditions of a stable water body system is simply that the potential energy in the system must be at a minimum. This means that a lighter water layer must be above a heavier water layer. The maximum water density is at 277°K and ρ will decrease with an increment of $|T-277|$.

There is a constant mechanism near the surface layer of a water body that develops the unstable stratification of the water density profile during the night and during winter and spring if there is no convective mixing mechanism introduced into the heat balance model. Of course, this is an unrealistic scenario, and in order to avoid this unrealistic situation, the full-depth convective mixing scheme proposed by Hostetler and Bartlein (1990) and Liston and Hall (1995a,b) is used in this model. The convective mixing scheme is based on the assumption that larger temperature instabilities will not exist in a freshwater body for any extended period of time. In this model, the configuration of temperature instabilities is eliminated by iteratively mixing the excess heat into adjacent "layers" of the water body until the between-layer temperature difference is less than a very small specified value (set to be zero in this model) (Hostetler and Bartlein, 1990). The convective mixing mechanism introduced in this model is very important, which is confirmed by a later comparison between the results with and without the convective mixing mechanism.

3. Numerical iteration scheme

Since Eqs. (2)–(4) are nonlinear equations, there is no analytical solution and only a numerical solution can be obtained. An entire water body can be delineated and divided into many layers. For both a deep (more than 50 m) or a shallow (more than 10 m and less than 50 m) water body, the surface layer is the thinnest, being less than 1 m because of the large temperature gradient and inclusion of several diurnal change issues. The thickness of other layers increases gradually with the depth of the layer. The first step was to develop a fine model with a total layer number of around 40 for a deep water body, and 20 for a shallow water body. In the following difference equations, Δz_j is the thickness of the layer j, and $m_{j,\text{total}}$ the total water equivalent mass in layer j, which is equal to $\rho_{\text{l}}.\Delta z_j$; and ρ_{l} is the liquid water density. $m_{i,\text{total}}$ consists of m_{ice} and m_{liq}, whose quantities depend on the h_j in the layer j.

Based on Eq. (2) and the definition (3a), the difference equation to determine h_j is given by Eq. (15a):

$$h_j(n+1,m+1)-h_j(n)= \frac{\Delta t}{\Delta z_j}\left\{\frac{(k+K)_{j+1/2}[T_{j+1}(n+1,m)-T_j(n+1,m)]}{z_{j+1}-z_j}-\frac{(k+K)_{j-1/2}[T_j(n+1,m)-T_{j-1}(n+1,m)]}{z_j-z_{j-1}}\right\}- \frac{\Delta t}{\Delta z_j}\left[\phi_{j+1/2}(n+1)-\phi_{j-1/2}(n+1)\right] . \quad (15a)$$

Using the definition for the enthalpy $h_{Lj}=h_j\Delta z_j$ in Δz_j, Eq. (15a) becomes:

$$h_{Lj}(n+1,m+1)-h_{Lj}(n)= \Delta t\left\{\frac{(k+K)_{j+1/2}[T_{j+1}(n+1,m)-T_j(n+1,m)]}{z_{j+1}-z_j}-\frac{(k+K)_{j-1/2}[T_j(n+1,m)-T_{j-1}(n+1,m)]}{z_j-z_{j-1}}\right\}- \Delta t[\phi_{j+1/2}(n+1)-\phi_{j-1/2}(n+1)] \quad (15b)$$

or:

$$h_{Lj}(n+1,m+1)-h_{Lj}(n)=\Delta t[Q_{j-1/2}(n+1,m)- Q_{j+1/2}(n+1,m)+\phi_{j-1/2}(n+1)-\phi_{j+1/2}(n+1)] , \quad (15c)$$

where:

$$\begin{cases} Q_{j-1/2}(n+1,m)=(k+K)_{j-1/2}\times \\ \quad [T_{j-1}(n+1,m)-T_j(n+1,m)]/(z_j-z_{j-1}) , \\ Q_{j+1/2}(n+1,m)=(k+K)_{j+1/2}\times \\ \quad [T_j(n+1,m)-T_{j+1}(n+1,m)]/(z_{j+1}-z_j) , \end{cases} \quad (16a)$$

$$\begin{cases} (k+K)_{j-1/2}= \\ \quad \dfrac{(k+K)_{j-1}\times(k+K)_j\times(\Delta z_{j-1}+\Delta z_j)}{(k+K)_{j-1}\times\Delta z_j+(k+K)_j\times\Delta z_{j-1}} , \\ (k+K)_{j+1/2}= \\ \quad \dfrac{(k+K)_{j+1}\times(k+K)_j\times(\Delta z_{j+1}+\Delta z_j)}{(k+K)_{j+1}\times\Delta z_j+(k+K)_j\times\Delta z_{j+1}} . \end{cases} \quad (16b)$$

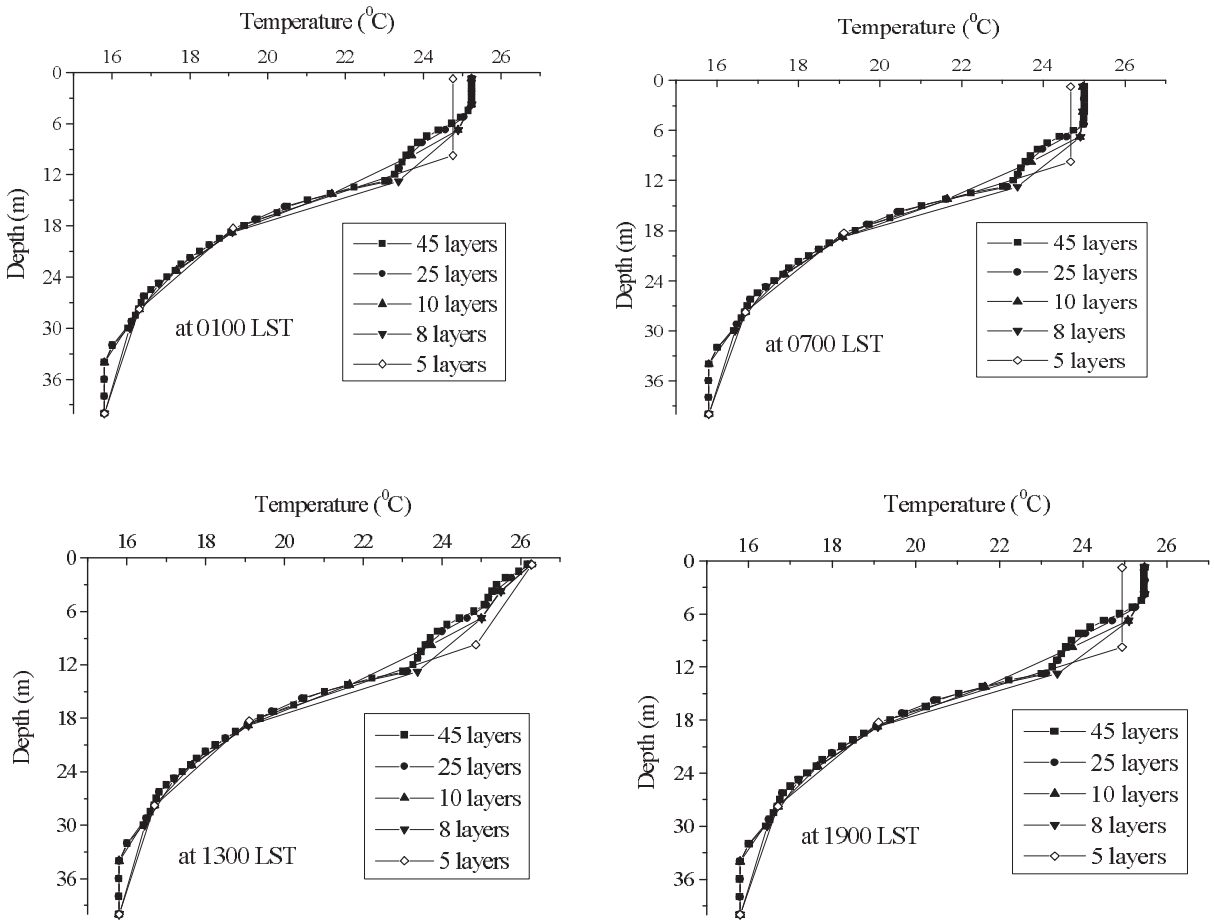

Fig. 4. Comparison of simulated temperature profiles with different numbers of layers at different times on day 10.

Boundary conditions are given by:

$$Q_{1/2}(n+1,m)=S_{\rm n}(n+1)+L_{\rm n}(n+1)-H_{\rm s}(n+1,m)- L_{\rm lv}E(n+1,m)+R_{\rm p}(n+1)\ , \quad (17a)$$

$$Q_{j+1/2}(n+1,m)=0\ , \quad (17b)$$

where $n+1$ and m indicates the time step and iteration step, respectively. The detailed iteration procedure to obtain $h_{Lj}(n+1,m+1)$ and then $T_j(n+1,m+1)$ and $f_{{\rm ice},j}(n+1,m+1)$ is given in Appendix A.

4. Results and discussion

4.1 *Model evaluation*

In order to evaluate the performance of the model developed here, two observed datasets of the non-frozen lake Kinneret in Israel (32.5°N, 35.4°E) from 21 May 2002 to 8 June 2002, and the frozen lake Lower Two Medicine in northern Montana, USA, from September 1992 to June 1993 were used. The first dataset includes atmospheric forcing data, such as air pressure, wind speed, air temperature, relative humidity, solar radiation, and downward longwave radiation from the atmosphere, as well as the temperature profile in the lake every 10 minutes. The second dataset, including the input of forcing data and the output of ice depth, is taken from Liston and Hall (1995a,b).

As examples, Figs. 1 and 2 show comparisons of temperature for the ice-free lake Kinneret between observed and simulated results at four typical instances on two randomly selected days. In these figures, the lines with ■ represent observed data and those with ▲ (with convection) represent the simulated data. It can be seen that the simulated results agree fairly well with the observed in both trend and magnitude. Statistically, the maximum and average absolute differences of simulated surface temperatures from the observed during the simulation period are 2.10 K and 0.44 K, respectively.

Figure 3 shows a comparison of total ice depth simulated by the model for the frozen lake Lower Two Medicine with observation data for nine months from September 1992 to June 1993. The average observed

Table 2. Statistics of temperature differences for different numbers of layers.

	Depth (m)	Average (K)	Maximum (K)
5 vs 45 layers	0.75	0.26	0.89
	9.75	0.95	1.70
	18.75	0.04	0.08
	27.75	0.01	0.02
	40	0.0	0.0
8 vs 45 layers	0.75	0.05	0.30
	3.75	0.17	0.67
	6.75	0.27	0.59
	12.75	0.33	0.61
	18.75	0.01	0.03
	24.75	0.0	0.0
	30	0.0	0.05
	40	0.0	0.0
10 vs 45 layers	0.75	0.04	0.29
	3.75	0.17	0.67
	6.75	0.26	0.57
	9.75	0.01	0.27
	14.25	0.03	0.07
	18.75	0.0	0.01
	23.25	0.02	0.04
	27.75	0.0	0.01
	34	0.0	0.0
	40	0.0	0.0
25 vs 45 layers	0.75	0.01	0.15
	3.75	0.05	0.24
	6.75	0.05	0.12
	9.75	0.06	0.13
	14.25	0.02	0.03
	18.75	0.0	0.0
	23.25	0.02	0.04
	27.75	0.02	0.03
	34	0.0	0.0
	40	0.0	0.0

depth is included along with the maximum and minimum observations for each observation time. As before, it can also be seen that the simulated ice depth and the average observed depth are in reasonably good agreement in both trend and magnitude, with the simulated ice depth consistently falling within the range of observed values. These good agreements for two datasets of non-frozen and frozen lakes mean the model developed here can describe the energy balance process in a water body such as a lake very well. A simplified model based on this more detailed model may therefore serve as an important and useful component within land surface models for climate study.

4.2 *Convective mixing mechanism*

As mentioned in the introduction, many previous models did not take the convective mixing mechanism into consideration for cases where the density in a layer is greater than that in its adjacent underlying layer. This situation occurs very often near the surface of a water body at night, and in the spring and winter seasons, when longwave radiation emitted from the surface layer or cold air temperature forces water to cool near the surface. This causes the placing of heavier water over lighter water and forms an unstable stratification distribution of water density. Therefore, a strong buoyancy force produces a strong mechanical convective mixing between the two layers and forces the two layers to be in equilibrium. The convective mixing process progresses very fast. In this model, as mentioned above, the full-depth convective mixing scheme proposed by Hostetler and Bartlein (1990) and Liston and Hall (1995a,b) is used in this model, which eliminates the configuration of temperature instabilities and establishes the equilibrium state between the two adjacent layers within every time step interval of 10 minutes. The reason to accept the above assumption is explained in Appendix B.

In Figs. 1 and 2, the simulated temperature profiles without considering the convective mixing process in the model is also included. It can be seen that there is always a turning point in the temperature profiles below the water surface from late evening to early morning. This point moves down from the surface in the evening to around 7 m deep the next early morning, and then disappears quickly due to the rapid increase of solar radiation penetration. Table 1 shows the statistics of temperature difference between two schemes with and without the convective mixing process. Maximum and average absolute temperature differences at the surface layer between the models with and without the mixing process reach 1.19 K and 0.32 K, respectively. Maximum and average absolute differences of latent heat fluxes from the water surface between the two model versions are 24.1 W and 9.0 W, and maximum and average absolute differences from the surface between the two sensible heat fluxes are 17.19 W and 2.4 W.

It is clearly shown from the figures that the profiles predicted by the model with the mixing mechanism follow the observed profiles much better than those without the mixing mechanism in either shape, trend, or magnitude. This indicates that the inclusion of the convective mixing mechanism is appropriate.

5. Model simplification: reducing the number of vertical layers

Water bodies such as lakes are one of the important underlying surfaces in current land surface models (LSMs) for climate system modeling. Modeling the climate system requires powerful computer resources,

Table 3. Statistics of latent heat flux and sensible heat flux differences for different numbers of layers.

Layers	Average latent heat	Maximum	Average sensible heat	Maximum
25 vs 45	0.59	9.43	0.16	2.68
10 vs 45	1.72	17.33	0.47	5.02
8 vs 45	1.80	17.38	0.50	5.02
5 vs 45	8.10	59.81	2.33	19.01

and thus the physical model and relevant numerical schemes of each component should be as simple as possible, while at the same time maintaining a high level of accuracy.

The results described in section 4.1 were predicted by the model with around 45 layers for the lake with a depth of around 50 m, and this takes up a large amount of computer time. The problem here is whether it is possible to greatly reduce the number of vertical layers but still maintain the same level of accuracy. What is the minimum possible number of layers for a water body with a depth of around 50 m?

Using the solution from the model with 45 layers as the standard, four substitutes of 25, 10, 8, and 5 layers were tested using the model. Figure 4 shows a comparison between the results from the schemes with less layers and the standard one. It can be seen that the more layers there are the better the agreement between simulated and observed data. However, it is also very clear that there are very small differences among the simulated results with 45, 25, 10, and 8 layers. The results when using 5 layers show a greater deviation from the standard. Tables 2 and 3 present a comparison of absolute maximum and average temperature, sensible heat, and latent heat between the simulated results using 5, 8, 10, and 25 layers, to those when using 45 layers. These also demonstrate that the results from 5 layers show a greater deviation from those using 45 layers. This means that a division of the water body into 10 layers is more acceptable than 5 layers.

6. Summary and conclusions

Based on the one-dimensional unsteady heat conduction equation, a model including the convective mixing function for studying the heat exchange between a water body and the atmosphere has been developed. The model with a detailed division was verified by observed data from Lake Kinneret and lake Lower Two Medicine, which demonstrated the ability to simulate the heat and mass exchange between the atmosphere and a water body is good. In order to use the model in climate studies, versions with less vertical division of the water body were tested and the results indicated that a division into around 10 layers can work as well as a more detailed division. From the numerical simulation study, the following conclusions can be drawn:

(1) A model using enthalpy instead of temperature as the predictive variable is more functional and effective, helping to set up precise equations, easily dealing with the phase change process, and simplifying the numerical scheme.

(2) Inclusion of the convective mixing mechanism in the model is very important. The simulated results with convective mixing were much better than those without.

(3) The numerical iteration scheme discussed in Appendix A is very effective for water bodies where a phase change process is involved.

Acknowledgements. Thanks to Prof. Moshe Gophen at the Kinneret Limnological Loboratory of Israel for providing the data from Lake Kinneret. Thanks to Prof. X. G. Gao for his useful suggestion to our research work. This work was supported by the National Natural Science foundation of China under Grant Nos. 40233034 and 40575043 and KZCX3-sw-229.

APPENDIX A

Equations (15) and (16) together with conditions (17) and constrains (4) are solved by using an iterative technique to obtain the solutions of $h_{L,j}, T_j$ and $f_{\mathrm{ice},j}$. The efficient methodology to solve Eqs. (15) and (16) iteratively is developed by this model as follows. Based on an estimated temperature profile $T_j(n+1,m)$, the $h_{Lj}(n+1,m+1)$ are obtained directly from Eqs. (15) and (16). In order to obtain the solutions of $T_j(n+1,m+1)$ and $f_{\mathrm{ice},j}(n+1,m+1)$ from the obtained $h_{Lj}(n+1,m+1)$, two important thresholds, h_{L1} and h_{L2}, of the enthalpy h_{Lj} should be defined here according to Eq. (4): (1) If all water in the layer j is in liquid phase and its temperature T_j is equal to freezing temperature T_{f}, the total enthalpy h_{Lj} must be equal to zero, that is $h_{L1} = 0$. (2) If all the water in the layer j is in ice phase and its temperature T_j is also equal to freezing temperature T_f, the total enthalpy h_{Lj} must be equal to $h_{L2} = -m_{j,\mathrm{total}} L_{il}$, which is equal to the energy absorbed by the phase change of total water mass $m_{j,\mathrm{total}}$ from complete ice to complete liquid water. By using the two thresholds h_{L1} and h_{L2}, the temperature $T_j(n+1,m+1)$ and ice

phase fraction $f_{\mathrm{ice},j}(n+1,m+1)$ for layer j will be easily determined by Eqs. (3b) or (3c) and (4) based on the obtained $h_{Lj}(n+1,m+1)$. There are three cases to decide the $T_j(n+1,m+1)$ and $f_{\mathrm{ice},j(n+1,m+1)}$, respectively. These are:

(1) If $h_{Lj}(n+1,m+1) > h_{L1} = 0.0$, the total water in the layer is in liquid phase and $f_{\mathrm{ice},j}(n+1,m+1) = 0.0$. $h_{Lj}(n+1,m+1)$ represents the thermal energy due to a temperature higher than T_{f}, and the temperature $T_j(n+1,m+1)$ is obtained by:

$$T_j(n+1,m+1) = \frac{h_{Lj}(n+1,m+1)}{m_{j,\mathrm{total}}c_j} + T_{\mathrm{f}} > T_{\mathrm{f}} \tag{A1}$$

where $m_{j,\mathrm{total}}$ is the total water mass in the layer j.

(2) If $h_{Lj}(n+1,m+1) < h_{L2}$, the total water in the layer is in ice phase and $f_j(n+1,m+1) = 1.0$. The difference between $h_{L2} - h_{Lj}(n+1,m+1)$ represents the thermal energy due to a temperature less than T_{f}, and the temperature will be given by:

$$T_j(n+1,m+1) = \frac{h_{Lj}(n+1,m+1) + m_{j,\mathrm{total}}L_{\mathrm{il}}}{m_{j,\mathrm{total}}c_j} + T_{\mathrm{f}} < T_{\mathrm{f}} \tag{A2}$$

(3) If $h_{L2} < h_{Lj}(n+1,m+1) < h_{L1}$, the water in the layer exists as a mixture of liquid and ice. The temperature of the mixture must be equal to T_{f} and the ice fraction, $f_{\mathrm{ice}}, j(n+1,m+1)$, of the total mass m_{total} can be estimated from the $h_{Li}(n+1,m+1)$ by:

$$m_{j,\mathrm{ice}} = -\frac{h_{Lj}(n+1,m+1)}{L_{\mathrm{il}}} \tag{A3a}$$

$$f_j(n+1,m+1) = \frac{m_{j,\mathrm{ice}}}{m_{j,\mathrm{total}}} \tag{A3b}$$

Final solutions for $h_{Lj}(n+1,m+1), T_j(n+1,m+1)$ and $f_{\mathrm{ice},j}(n+1,m+1)$ are iteratively obtained if $|T_j(n+1,m) - T_j(n+1,m+1)| < \varepsilon$ where ε is the criterion for solution convergence. Finally, the fractional masses $m_{j,\mathrm{liq}}$ and $m_{j,\mathrm{ice}}$ of $m_{j,\mathrm{total}}$ can be calculated from the final $f_{\mathrm{ice},j}(n+1)$.

APPENDIX B

If the density in the top layer is greater than that in the adjacent layer below, the density difference $\Delta\rho$ between the two layers is decided by the temperature difference ΔT between the two layers. According to the relation of density ρ with temperature T:

$$\rho = (1 - 1.9549 \times 10^{-5}|T - 277|^{1.68})10^3 ,$$

the density difference $\Delta\rho$ is equal to:

$$\Delta\rho = 1.9549 \times 10^{-5}(|T_1 - 277|^{1.68} - |T_2 - 277|^{1.68})10^3$$

$$\approx 1.9549 \times 10^{-5}|T_1 - 277|^{1.68} \times 1.68 \left|\frac{\Delta T}{(T_1 - 277)}\right| 10^3$$

$$\approx 1.9549 \times 1.68 \times 10^{-5}|(T_1 - 277)^{0.68} \times \Delta T|10^3 .$$

Then, the downward buoyancy force F for mass ρ in the top layer is:

$$F \approx \Delta\rho \times g \approx 3.3 \times 10^{-2} \times g|(T_1 - 277)^{0.68} \times \Delta T|$$

and the acceleration velocity a (m s^{-1}) of a parcel with the mass ρ (≈ 1000 kg m^{-3}) is:

$$a = F/\rho$$
$$\approx 0.033 \times g|(T_1 - 277)^{0.68} \times \Delta T|/\rho$$

Therefore, the subsidence distance S of the parcel in time interval Dt is:

$$S \approx 0.5 \times a \times Dt^2 .$$
$$= 0.00015|(T_1 - 277)^{0.68} \times \Delta T| \times Dt^2 .$$

If Dt=900.0 s and $|(T_1 - 277)^{0.68} \cdot \Delta T)| \approx |\Delta T|$,

$$S \approx 0.00015 \times 900 \times 900\Delta T \approx 120\Delta T$$
$$\approx 120 \text{ m for } \Delta T = 1 \text{ K} ,$$
$$\approx 12 \text{ m for } \Delta T = 0.1 \text{ K} ,$$
$$\approx 1.2 \text{ m for } \Delta T = 0.01 \text{ K} .$$

This means the convective turnover mechanism in ΔT time is enough to make the two adjacent layers mixed.

REFERENCES

Bell, V. A., D. G. George, R. J. Moore, and J. Parker, 2006: Using a 1-D mixing model to simulate the vertical flux of heat and oxygen in a lake subject to episodic mixing. *Ecological Modelling*, **190**, 41–54.

Bonan, G. B., 1996: A land surface model (LSM version 1.0) for ecological, hydrological and atmospheric studies: Technical description and user's guide, NCAR Technical Note, NCAR/TN-417+STR, National Center for atmospheric Research, Boulder, CO., USA, 150pp.

Businger, J. A., J. C. Wyngard, and Y. Izumi, 1971: Flux-profile relationships in the atmospheric surface layer. *J. Atmos. Sci.*, **28**(2), 181–189.

Dickinson, R., and Coauthors, 1993: Biosphere Atmosphere Transfer Scheme (BATS) version 1E as coupled to the NCAR community Climate Model. NCAR, Tech Note. NCAR-387+str, 72pp.

Dyer, A. J., 1974: A review of flux-profile relations. *Bound.-Layer Meteor.*, **1**, 363–372.

Fang, X., and H. G. Stefan, 1996: Long-term lake water temperature and ice cover simulations/measure ments. *Cold Regions Science and Technology*, **24**, 289–304.

Henderson-Sellers, B., 1985: New formulation of eddy diffusion thermocline models. *Applied Mathematical Modeling*, **9**, 441–446.

Henderson-Sellers, B., 1986: Calculating the surface energy balance for lake and reservoir modeling: A review. *Rev. Geophys.*, **24**(3), 625–649.

Hostetler, S. W., 1991: Simulation of lake ice and its effect on the late-Pleistocene evaporation rate of lake Lahontan. *Climate Dyn.*, **6**, 43–48.

Hostetler, S. W., and P. J. Bartlein, 1990: Simulation of lake evaporation with application to modeling lake level variations of Harney-Malheur Lake, Oregon. *Water Resour. Res.*, **26**(10), 2603–2612.

Liston, G. E., and D. K. Hall, 1995a: An energy-balance model of lake-ice evolution. *J. Glaciol.*, **41**(138), 373–382.

Liston, G. E., and D. K. Hall, 1995b: Sensitivity of lake freeze-up and break-up to climate change: a physically based modeling study. *Annals of Glaciology*, **21**, 387–393.

Oleson, W. K., and Coauthors, 2004: Technical description of the Community land model (CLM). NCAR Technical Note, NCAR/TN-461+STR National Center for atmospheric Research, Boulder, CO., USA, 174pp.

Patrick, M., C. R. Duguay, G. M. Flato, and W. R. Rouse, 2002: Simulation of ice phenology on Great Slave Lake, Northwest Territories, Canada. *Hydrological Processes*, **16**, 3691–3706.

Patterson, J. C., and P. F. Hamblin, 1988: Thermal simulation of a lake with winter ice cover. *Limnology Oceanography*, **33**(3), 323–338.

Sellers, P. J., Y. Mintz, Y. C. Sud, and A. Dalcher, 1986: A simple biosphere model (SIB) for use within general circulation models. *J. Atmos. Sci.*, **43**, 505–531.

Stefan, H. G., and X. Fang, 1997: Simulated climate change effects on year-round water temperature in temperature zone lakes. *Climatic Change*, **40**, 547–576.

Sun, S. F., J. Jin, and Y. K. Xue, 1999: A simple snow-atmosphere-soil transfer model. *J. Geophys. Research*, **104**, No. D16, 19587–19597.

Vavrus, S. J., R. H. Wynne, and J. A. Foley, 1996: Measuring the sensitivity of southern Wisconsin lake ice to climate variations and lake depth using a numerical model. *Limnology and Oceanography*, **41**(5), 822–831.

Zhou, C. Z., and S. C. Chapra, 1997: The simulation of lake thermal constitution and evaporation. *Environment Science*, **15**(2), 33–37. (in Chinese)